

Binary Lenses in OGLE-II 1997–1999 Database. A Preliminary Study

M. J a r o s z y ń s k i

Warsaw University Observatory, Al. Ujazdowskie 4, 00-478 Warszawa, Poland
e-mail:mj@astrouw.edu.pl

ABSTRACT

We present 18 binary lens candidates from OGLE-II database for seasons 1997–1999. The candidates have been selected by visual light curves inspection from the subsample of strong transient events; the same procedure gives 215 single lens candidates. Among the double lenses there are 12 cases interpreted as caustic crossing events. We compare the mass ratio and separation distributions obtained for binary lenses with the predictions based on stellar double systems observations. We take into account the selection bias, which causes over-representation of binary lenses of similar mass and separation close to the Einstein radius. There is no strong discrepancy between the expected and observed distributions of the mass ratio or the binary separations. We find one or two cases of binary lens candidates, SC20_1793 and SC20_3525, with extreme mass ratios, which may suggest presence of planets or brown dwarf companions. Unfortunately, neither case is very strong, as alternative solutions provide fits to the data which are only unsubstantially worse. Binary lenses provide a modest contribution to overall optical depth to microlensing.

galaxies: individual (Milky Way) – gravitational lensing

1. Introduction

As estimated by Mao and Paczyński (1991) several percent of all microlensing events in our Galaxy should be caused by binaries acting as lenses. The first such case, the event OGLE-7 (Udalski *et al.* 1994a) was analyzed also by Dominik (1999), who showed the existence of several different binary lens models of the event.

The amount of information one may obtain from a binary lens light curve depends strongly on the frequency of observations and the kind of the event itself. The events with well sampled caustic crossing may be used to study the effect of limb darkening in the atmospheres of lensed stars (*e.g.*, Albrow *et al.* 1999b) or to set limits on the source velocity relative to the lens (*e.g.*, Albrow *et al.* 1999a). In some cases with caustic crossings and a pronounced effect of Earth motion parallax, the mass of the lens can be found (An *et al.* 2001). Such finding is not possible for single gravitational lenses and rather uncommon for doubles. The typical caustic crossing takes several hours, and the observations should be taken every ten or twenty minutes to be useful for detailed modeling. The standard frequency of observations used by the gravitational lens survey teams (including OGLE-II – Udalski *et al.* 2000) is one or two per night – insufficient to treat the caustic crossings as separate issue. Some properties of binary lenses can be found even without well sampled caustic crossings.

The only systematic study to date of the binary lens population was made for the MACHO data (Alcock *et al.* 2000). It gives the light curves and binary lens models for 21 events observed in 1993–1998. Many of the events were known to be caused by binary lenses early enough to make the follow up observations with the dense sampling of the caustic crossing. In four cases the relative proper motion of the lens was measured with the accuracy sufficient to study the likelihood of the lens masses. The distribution of the binary mass ratio is also given.

Woźniak *et al.* (2001) present a list of 520 gravitational lens candidates among OGLE-II stars based on the new data processing using DIA photometry (Alard and Lupton 1998, Alard 2000). The database includes observations of seasons 1997–1999. Most of the candidates have been found algorithmically. The list is supplemented by candidates selected by visual inspection of the light curves and also by some events which were known as candidates in earlier study (Udalski *et al.* 2000). The sample of the gravitational lens candidates belongs to a larger sample of transient sources. The transient sample (Woźniak 2000, Woźniak *et al.* 2001) has been selected in fully algorithmic manner from all OGLE-II light curves and serves as the basis of the present study.

Our goal is to find the candidates for binary lens events, find their models and make some survey of the binary lens population properties. In the next Section we describe our selection method for finding both single and binary lens candidates in the transient sample of Woźniak *et al.* (2001). In Section 3 we describe the procedure of fitting binary lens models to the data. The results are described in Section 4, while the graphical material is shown in Appendix. Discussion follows in Section 5.

2. Choice of Candidates

Woźniak (2000) and Woźniak *et al.* (2001) describe the construction of the transient sample based on OGLE-II data for seasons 1997–1999 processed using the DIA photometry. The sample contains 4424 sources. The transients are selected algorithmically, as sources which have (almost) constant flux of radiation and undergo at most two brightening episodes during observation span. We follow Woźniak in defining a threshold value for physical flux variation. We assume that the variability of the source is limited to a sequence containing not more than 50% of all observations. The remaining data points serve to define a constant flux base. The choice of the “variable” part is made in a way minimizing the scatter of the remaining observations (the “base”). We calculate σ_{base} – a *rms* deviation of flux measurements from its mean value F_{base} . Following Woźniak (2000) we adjust the calculated parameter taking into account possibly non-Gaussian distribution of flux values around the mean. Finally, we obtain the threshold parameter $\delta = \max\{\sigma_{\text{base}}, \sigma_{\text{ph}}\}$, where σ_{ph} is the mean photometric error estimated for the points belonging to the constant flux database. Woźniak *et al.* (2001) define a brightening episode as 3 consecutive points at least 5δ above the base flux or 4 points at least 4δ above.

The light curves of binary lens events usually have two maxima and it is necessary to have at least five measurements to distinguish them. For this reason and having in mind some safety margin, we require the transients to have at least 7 points which are 5δ above the base flux. Some experience with Woźniak *et al.* (2001) database suggests an extra criterion for selecting the interesting events, which helps removing DIA photometry artifacts from the investigated light curves. In further investigation we include only the light curves with at least 7 points which are 5δ above the base flux with at least one point among them at 15δ level.

Using our criteria we automatically search the transient database getting 390 light curves. We visually inspect all the selected cases. For each light curve we try a single lens fit taking into account blending. In the majority of cases comparison of the best single lens fit with the data shows a good agreement, in the sense of visual impression and the χ^2 value. There are cases of weak transients, which can be formally fitted with single lens model based on χ^2 value, which are nevertheless rejected after visual inspection, usually the changes in flux look as random with a period of increased mean flux value. There are also cases which under visual inspection show a very good agreement with a single lens model light curve, but have high χ^2 value. Usually these are the strongest lensing events. We treat them as single lens events not investigating further the reasons for low formal quality of the fits. The second most common category among selected transients are artifacts of DIA photometry. They show irregular behavior dominated by noise. In many cases series of sources close to each other show very similar light curves of this kind. In a few cases the light curves suggest periodic variability. We exclude the possibility that there are binary lenses belonging to this category. The binary lens candidates are chosen mostly on the basis of visual inspection. Some show the characteristic “U-shape” of the caustic crossing. Some have multiple flux maxima. The other show asymmetry. All visually selected candidates have high values of χ^2 for a single lens model, usually exceeding 3 per degree of freedom. There are also several cases of good quality light curves, which do not resemble a single or binary lens model variability. We put them into “other objects” category.

Among 390 transient selected we find 215 single lenses and 141 unclassifiable cases of poor photometry. We treat 27 of the remaining 34 light curves as possible binary lens candidates, and 7 – as “other objects”.

3. Fitting Binary Lens Models

The models of the two point mass lens were investigated by many authors (Schneider and Weiss 1986, Mao and DiStefano 1995, DiStefano and Mao 1996, Dominik 1998, to mention few). The methods applicable for extended sources have recently been described by Mao and Loeb (2001). While we use mostly the point source approximation, we extensively employ their efficient numerical schemes for calculating the binary lens caustic structure and source magnification.

We fit binary lens models using the χ^2 minimization method for the light curves. It is convenient to model the flux at the time t_i as:

$$F(t_i) = F_b + F_s \times A(t_i) \equiv F_{\text{base}} + F_s \times (A(t_i) - 1) \quad (1)$$

where F_b is the blended flux (from the source close neighbors and possibly the lens), F_s – the flux of the source which is lensed, and $A(t_i)$ is the lens magnification. The combination $F_{\text{base}} \equiv F_b + F_s$ is the total flux long before or long after the event. The DIA photometry only gives the flux differences, so one can use $\tilde{F}_i \equiv F_i - F_{\text{base}}$ as “measured” quantities. Using this notation one has for the χ^2 (Woźniak 2000):

$$\chi^2 = \sum_{i=1}^N \frac{\left((A_i - 1)F_s - \tilde{F}_i \right)^2}{\sigma_i^2} \quad (2)$$

where σ_i are the errors of the flux measurement taken from the DIA photometry. For self-consistency we check the value of χ^2 calculated for the points defining the constant flux base.

Binary lens models are possibly and typically non unique (Dominik 1999). The presence of caustics and cusps in the lens theory (Schneider, Ehlers and Falco 1992, Blandford and Narayan 1992) makes the χ^2 dependence on the model parameters complicated and discontinuous for point sources. This suggests that the search for the χ^2 global minimum may be difficult because of the likely existence of many local ones. For this reason we combine the scan of the parameter space with the standard minimization techniques in our search.

The light curves we investigate do not have well sampled caustic crossings, so we use the point source model in the majority of calculations. For the same reason we are also not able to use the strategy of Albrow *et al.* (1999c) for finding binary lens models. We also neglect the parallax and/or binary rotation effects, which further simplifies the models.

The binary system consists of two masses m_1 and m_2 , where by convention $m_1 \leq m_2$. The Einstein radius of the binary lens is defined as:

$$r_E = \sqrt{\frac{4G(m_1 + m_2)}{c^2} \frac{d_{OL}d_{LS}}{d_{OS}}} \quad (3)$$

where G is the constant of gravity, c is the speed of light, d_{OL} is the observer–lens distance, d_{OS} is the observer–source distance, and d_{LS} is the distance between the lens and the source. The Einstein radius serves as a length unit and the Einstein time: $t_E = r_E/v_{\perp}$, where v_{\perp} is the lens velocity relative to the line joining the observer with the source, serves as a time unit. The passage of the source in the lens background is defined by seven parameters: $q \equiv m_1/m_2$ ($0 < q \leq 1$) – the binary mass ratio, d – binary separation expressed in r_E units, β – the angle between the source trajectory as projected onto the sky and the projection of the binary axis, b – the impact parameter, t_0 – the time of closest approach of the source to the binary center of mass, t_E – the Einstein time, and F_s the (not

magnified) source flux. For all other parameters fixed, F_s can be obtained from the (linear) equation $\partial\chi^2/\partial F_s = 0$ with the obvious limitation $0 \leq F_s \leq F_{\text{base}}$. Thus we are left with the six dimensional parameter space to look for minima. We begin with a scan of the parameter space using a logarithmic grid of points in (q, d) plane ($10^{-3} \leq q \leq 1$, $0.1 \leq d \leq 10$) and allowing for continuous variation of the other four parameters (inclusion of q and d , which change the caustic structure of the binary, in the automatic routine finding χ^2 minimum may cause problems with its convergence – see An *et al.* (2001) Jaroszyński and Mao (2001)). The other dimensions are searched using AMOEBA routine (Press *et al.* 1992). We use many starting points in (β, b, t_0, t_E) subspace. The expected value for the Einstein time t_E is based on the event duration. The expected time of the closest approach to the binary center of mass t_0 should be close to the time of the maximal observed flux. The direction of the source motion relative to the binary axis β is chosen at random. For each choice of β there is a defined range of impact parameter b giving rise to a “binary character” of the light curve. Practically it means that the source should either cross a caustic or pass not too far from it.

Using the point source approximation we find the best binary lens models for every (q, d) on the grid. With the fitted value of the Einstein time t_E and the typical velocity of a source relative to the observer–lens line v , we are able to estimate the linear size of the Einstein radius as projected into the source plane $\tilde{r}_E \approx vt_E$. The fitted deblended source flux allows for a crude estimate of the star radius R_s , and corresponding dimensionless source radius $r_s \equiv R_s/\tilde{r}_E$. For self consistency we repeat the fitting procedure at every grid point using the extended source model of the estimated size and starting from the solution obtained in the point source approximation. Finally we search the regions of (q, d) plane with the lowest values of χ^2 on a finer grid.

4. Results

We have applied the fitting procedure to the 27 selected events. We also visually compare the top quality models with the data, checking whether the fitted light curves are “natural”, not having superficial peaks in places not covered by observations. In eighteen cases the binary lens fits are formally good and natural. They are also substantially better than single lens fits applied to the same data (the binary fits give the χ^2 values lower at least by 50, and typically by several hundreds or more as compared with single lens fits.) There are three candidates with formally good fits which are rejected after the visual inspection of the models. The other six are rejected because of the high χ^2 value. The plots showing light curves and our best fits for the rejected candidates are included in Appendix.

Nine of the events are on the Udalski *et al.* (2000) list of microlensing events, and five of them were detected in real time and included in the alerts of the Early Warning System (Udalski *et al.* 1994b). One of the events (SC21_6195) has been included in Alcock *et al.* (2000) study of binary lenses as candidate

event 97-BLG-d2. Not all events marked as possible binary lens candidates by Udalski *et al.* (2000) are on our list. We give the comparison of the two lists in the Section 5.

4.1 The Binary Lens Models

Of the eighteen binary lens candidates, twelve show caustic crossing, five at least one close cusp approach with sharp light maximum, and one has two shallow maxima explained by passages at greater distances from cusps.

Table 1
Binary microlensing events

Field	Identification		EWS	RA (2000)	DEC (2000)	I_0 [mag]
	DIA	OGLE				
BUL_SC3	7390	792295	1998-BUL-28	17 ^h 53 ^m 54 ^s .14	−29°36′40″.8	19.461
BUL_SC4	6350	-	-	17 ^h 54 ^m 47 ^s .47	−29°34′19″.4	19.229
BUL_SC5	6550	-	-	17 ^h 50 ^m 51 ^s .52	−29°34′11″.6	16.177
BUL_SC12	997	-	-	18 ^h 15 ^m 59 ^s .02	−24°10′04″.8	19.605
BUL_SC15	1631	373196	-	17 ^h 48 ^m 07 ^s .05	−23°12′03″.2	19.527
BUL_SC16	1047	32304	-	18 ^h 09 ^m 38 ^s .47	−26°32′26″.8	18.422
BUL_SC18	4924	-	-	18 ^h 06 ^m 54 ^s .66	−26°54′02″.8	18.541
BUL_SC19	668	26606	1999-BUL-23	18 ^h 07 ^m 45 ^s .14	−27°33′15″.2	17.868
BUL_SC20	1793	-	-	17 ^h 59 ^m 02 ^s .69	−29°03′03″.0	15.377
BUL_SC20	3525	708586	1999-BUL-25	17 ^h 59 ^m 41 ^s .14	−28°47′18″.4	18.329
BUL_SC20	4694	-	-	17 ^h 59 ^m 14 ^s .40	−28°36′55″.6	19.083
BUL_SC21	6195	833776	(97-BLG-d2)	18 ^h 00 ^m 39 ^s .58	−28°34′43″.3	17.721
BUL_SC30	4491	-	-	18 ^h 01 ^m 44 ^s .29	−28°41′30″.0	18.576
BUL_SC31	1795	293442	1999-BUL-17	18 ^h 02 ^m 22 ^s .50	−28°40′43″.9	18.638
BUL_SC31	3204	-	-	18 ^h 02 ^m 17 ^s .56	−28°24′10″.1	19.643
BUL_SC32	4683	-	-	18 ^h 02 ^m 57 ^s .13	−28°12′53″.3	17.241
BUL_SC35	2526	305604	-	18 ^h 04 ^m 22 ^s .42	−27°57′52″.2	18.905
BUL_SC36	4030	336761	1999-BUL-11	18 ^h 05 ^m 29 ^s .59	−27°59′14″.3	18.537

Note: The event identification consists of the OGLE field number, the star number in DIA database, and optionally of OGLE star number and EWS event name. The other columns give the star position (α , δ), and the base magnitude in the I -band.

In Table 1 we give the names, positions and observed magnitudes in I band of the objects long before or long after the event.

In Table 2 we give the parameters for the best models of each of the events. In some cases we include also another solution if it belongs to a distinct χ^2 minimum and lies inside the confidence region. Our best fits are also shown on the plots in Appendix. For each binary there are three separate plots. The first shows the source trajectory as projected onto the lens plane with caustic structure and binary components included. The model light curves and observed

fluxes are shown in the second plot. The third diagram shows the χ^2 confidence regions in the $\lg q$ - $\lg d$ plane.

Table 2
The binary lens models parameters

Field	DIA	$\chi^2/\text{d.o.f.}$	q	d	β	b	t_0	t_E	f	r_s
SC3	7390	309.6/288	0.452	0.376	132.07	0.10	1067.4	113.5	0.99	0.0006
SC4	6350	259.4/272	0.306	0.902	115.82	-0.30	1376.3	71.3	0.36	0.0006
		261.6/272	0.631	1.259	126.15	0.07	1376.2	66.2	0.27	0.0005
SC5	6550	278.3/272	0.966	0.881	76.05	0.01	615.2	24.6	0.01	0.0011
SC12	998	157.4/180	0.543	0.462	102.85	-0.09	1398.7	26.6	0.33	0.0011
SC15	1631	179.2/192	0.197	1.012	151.46	0.14	578.9	7.8	0.59	0.0058
SC16	1048	217.5/183	0.507	1.641	194.24	-0.21	565.6	27.7	0.36	0.0023
SC18	4924	156.2/194	0.292	1.084	18.94	-0.48	1217.9	89.1	0.44	0.0007
SC19	667	206.5/175	0.216	2.483	73.13	1.65	1346.6	58.8	0.94	0.0027
SC20	1793	133.9/225	0.017	2.917	144.03	1.25	632.6	6.7	0.96	0.1003
		134.2/225	0.501	0.355	319.24	-1.29	615.9	6.3	0.95	0.1045
SC20	3525	137.5/196	0.009	0.684	82.03	-0.02	1336.6	77.8	0.14	0.0004
		137.8/196	0.010	1.413	82.57	-0.03	1331.7	67.6	0.16	0.0005
SC20	4695	144.7/222	0.495	0.582	246.83	-0.08	586.8	108.2	0.08	0.0002
		145.0/222	0.822	0.861	205.26	0.27	577.9	63.6	0.28	0.0006
SC21	6195	206.1/223	0.543	1.135	104.33	-0.35	601.9	56.3	0.46	0.0019
SC30	4491	144.6/197	0.150	0.638	219.77	-0.11	1448.5	74.0	0.23	0.0006
SC31	1795	172.9/226	0.193	1.303	83.01	0.51	1310.3	18.9	0.75	0.0046
SC31	3205	228.7/225	0.106	0.750	347.39	-0.06	1271.9	78.3	0.17	0.0003
SC32	4683	150.8/198	0.176	1.274	54.72	-0.19	1146.4	243.6	0.04	0.0001
SC35	2526	140.0/169	0.785	0.442	304.50	-0.07	682.5	105.9	0.35	0.0004
		140.1/169	1.000	2.818	29.70	0.71	821.0	119.9	0.54	0.0005
SC36	4030	182.3/180	0.292	1.462	63.14	0.46	1300.4	94.7	0.45	0.0007

The source radius r_s in Einstein units, which we give in the last column is not a fitted parameter. It is only estimated and used for the self consistency check.

We concentrate mostly on the physical parameters of the binary (q and d). Examining the plots one can see that not all events can be well constrained and for some the 1σ confidence regions are rather large and irregular.

4.2 Distribution of Mass Ratios and Separations

There are 12 caustic crossing binary lens events among the total of 18. The conditional probability of a binary lens to cause a caustic crossing event is well defined (Mao and Paczyński 1991). It is proportional to the angle averaged width of caustic measured in the direction perpendicular to the source path and can be calculated for any binary lens as $w(\lg q, \lg d)$, where we use the dependence on logarithms as more convenient. The most efficient lenses have $q \approx 1$ and $d \approx 1$.

The rate of observed caustic crossing events caused by lenses with given parameters $P_{\text{BCC}}(\lg q, \lg d)$ also depends on the distribution of binary stars parameters $P_{\text{bin}}(\lg q, \lg d)$. Following Mao and Paczyński (1991) we assume, that the uniform distribution of binary systems in the logarithm of orbital period, which holds over six decades (Abt 1983) translates into uniform distribution in the logarithm of semimajor axis, and consequently in $\lg d$. Under this assumption the distribution of parameters among observed events is given by:

$$P_{\text{BCC}}(\lg q, \lg d) \sim P_{\text{bin}}(\lg q)w(\lg q, \lg d) \quad (4)$$

and, in principle, may be used to constrain $P_{\text{bin}}(\lg q)$. The binary systems database has been investigated by Trimble (1990), who shows that the mass ratio distribution is uniform in $\lg q$. This dependence is not valid for small q where the binaries are less abundant. We consider distributions of the form:

$$P_{\text{bin}}(\lg q) \sim \begin{cases} q/q_0 & q \leq q_0 \\ 1 & q \geq q_0 \end{cases} \quad (5)$$

using $0.03 \leq q_0 \leq 0.3$ which defines the location of the power law break. Using the above formulae one can find the integral probability distribution for the mass ratio and separation among the binaries causing BCC events. It is not obvious how to model the probability distribution for the cases without caustic crossings. We assume that our calculation, which includes only the caustic crossing events, may be applied to a sample including both caustic crossing and cusp approach events. The comparison of the theoretical predictions with the distribution of the binary lens sample, excluding the event 1998-BUL-28, which shows no sharp feature in the light curve. is shown in Fig. 1.

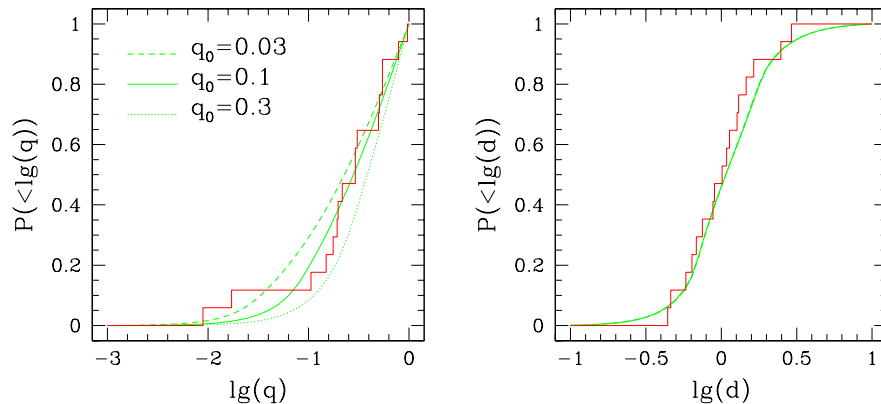


Fig. 1. Integral probability distributions for the mass ratio (left) and the binary separation (right) as compared with the binary lens sample. Curves corresponding to the same limiting mass ratio values ($q_0 = 0.03-0.3$) are shown on both plots, but the curves on the right panel are indistinguishable. (See the text for details on binary star population modeling.)

Our binary sample consists of the best models for each event. There are two cases with extreme mass ratios: SC20_1793 and SC20_3525. Both are cusp approach events. The first of the cases has also many other fits within the 1σ confidence limits with $q > 0.1$. The other case is a more serious candidate for an extreme mass ratio binary lens, but models with $q > 0.1$ are present within 2σ confidence limits.

The mass ratio and separation distributions of our sample (excluding possible extreme cases) is in rough agreement with theoretical expectations. The number of cases is low, so it is too early to make definite conclusions regarding the distribution of parameters among the binary stars.

4.3 Distribution of Einstein Radius Crossing Time

The Einstein radius crossing time is a physical parameter depending on the distances, lens mass and relative velocity, which can be found both for single and binary lenses. We show the histogram of this quantity for our sample of binary lens candidates in Fig. 2.

The statistics is poor, but the over-representation of the long lasting events, as compared with our single lens sample is apparent. The binary lenses should be twice as massive on average, which translates to the $\sqrt{2}$ factor in Einstein time. This is, however, not sufficient to explain the difference between the distributions.

4.4 The Blending Parameter f

This parameter, showing the fraction of the base flux belonging to the lensed star (while the rest is blended) can be fitted with greater confidence than for single lenses. We force this parameter to belong to the region $0.01 \leq f \leq 0.99$. Only one of our models lies on its upper boundary. (Sometimes one can obtain unphysical solutions with $f > 1$ and low χ^2 value which represent blends of negative fluxes. Other rather unlikely models can have $f \rightarrow 0$ and very high amplification – usually related to crossing of a small caustic. None of our models falls into the second category.) We show a histogram of f values in Fig. 3.

For better comparison of single and binary lens models we show their positions on $\lg(t_E)$ – f diagram. We use the convention employed also by Woźniak *et al.* (2001), which preserves single lens fits with unphysical values of blending parameter ($f > 1$) implying the negative flux of light from the blend. (If forced to $f \leq 1$, these models cluster on the boundary of permitted region.) Another unphysical region on the diagram consists of points with $f \rightarrow 0$ and high t_E . The presence of single lens models in the unphysical regions of the diagram is explained by Woźniak and Paczyński (1997) and is related to the degeneracy among fitted parameters in certain situations.

In Fig. 4 we show the single and binary lens models belonging to our sample. The median points for the two kinds of lenses are different: the binaries have systematically longer duration (73^d versus 30^d for singles) and are more blended ($f_{\text{med}} = 0.36$ versus 0.62 for singles). It is interesting to point out that for all of

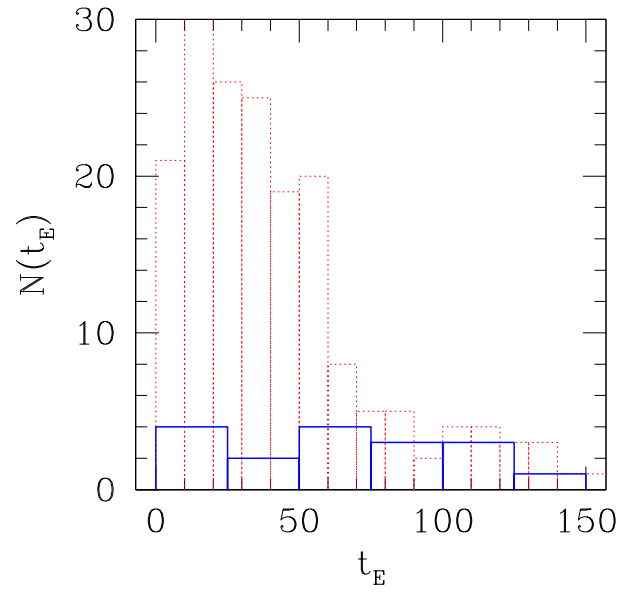


Fig. 2. Distribution of the Einstein radius crossing time t_E for the sample of binary lenses (solid line) as compared with the sample of single lenses (dotted) selected from the transient database using the same criteria.

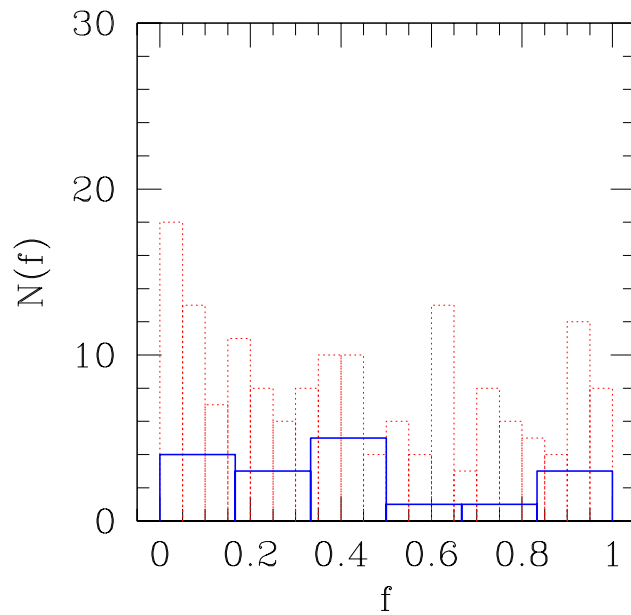


Fig. 3. Distribution of the parameter f defining which part of the base flux belongs to the source. (Part proportional to $1 - f$ belongs to stars close to the source and to the lens *i.e.*, the blends.) The histogram for binary lenses (solid) is compared with the histogram for our single lens sample (dotted).

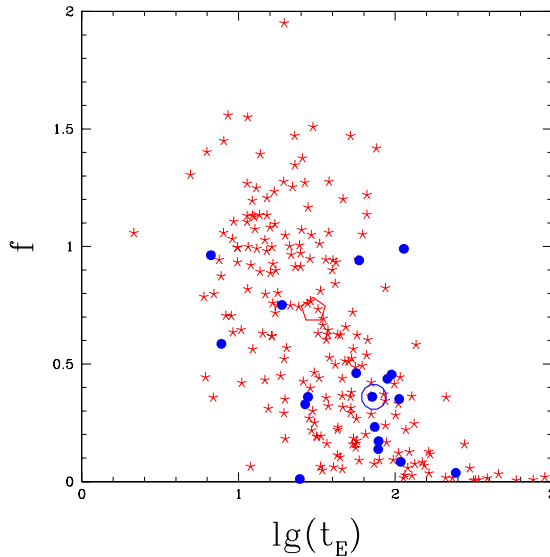


Fig. 4. Positions of binary (dots) and single (stars) lens models on the $\lg(t_E)$ - f diagram. The median points for binaries (open circle) and singles (open pentagon) are also shown.

the 520 single lenses of Woźniak *et al.* (2001) the median duration is even shorter (23^d) and the blending less important ($f_{\text{med}} = 0.88$). The simple rejection of all models with $f > 1$ gives almost equal values of median blending parameters ($f_{\text{med}} \approx 0.37$) for binaries, singles from our sample and singles from Woźniak *et al.* (2001). The median Einstein times become longer for $f < 1$ subsamples of single lens models, but still shorter than for binaries ($42^d/33^d$ versus 73^d). There is no simple criterion for removing models with $f \rightarrow 0$ and we do not pursue this issue.

4.5 Contribution of Binary Lenses to Microlensing Optical Depth

Gravitational microlensing is detected because of the temporary presence of an extra flux of light caused by source amplification. The detailed modeling of the detection process is a separate issue, but it is clear that both the duration of the event and the strength of the lens play here important roles. The customary definition of lensing event (Paczynski 1996) requires the object to be amplified at least 1.34 times, which corresponds to the source position inside the Einstein ring. Thus the contribution of a single event to the optical depth is proportional to the time it spends above the threshold amplification. For a blended source the observed amplification is not so simply related to the lens position. In DIA photometry it is rather the flux difference, which is important in discovering lensing events. We estimate the relative contribution of binary and single events to the microlensing optical depth comparing the extra light related to the two

kinds of phenomena. The extra light corresponding to a particular event is given as:

$$a_i = F_s \int (A_i(t) - 1) dt \quad (6)$$

where index i enumerates the events. Comparing the whole extra light of our binary lenses with the extra light of single lenses we obtain:

$$\frac{\sum_{\text{bin}} a_i}{\sum_{\text{sin}} a_i} = 0.03 \quad (7)$$

which suggests a 3% contribution of binary lenses to optical depth. The base fluxes of objects belonging to our sample which undergo single lensing are systematically higher than for objects undergoing binary lensing. This may be the result of our selection criteria. The effect diminishes the importance of binary lenses. It is possible that sources amplified by binary lenses are on average fainter as compared to sources undergoing lensing by single masses for a wide class of selection criteria. We check also other possibilities using our sample of single and binary lenses but changing the population of sources. This should be treated as a thought experiment which serves only to estimate the likely systematic errors of the above result – it is not guaranteed that for a different population of sources the same population of lenses would be discovered.

In the first experiment we assume that the base flux (F_{base}) of all objects is the same. We keep unchanged the other parameters of the lens models (including f). Calculating the ratio of extra light contributed by binary and single lenses we obtain the value 0.11. In the second experiment we assume that the source fluxes (F_s) are the same for all objects. This gives 0.05 for the calculated ratio.

The preliminary analysis of our sample shows that the recognizable binary lenses make about 8% of all lensing events in excellent agreement with Mao and Paczyński (1991). Estimating the contribution to optical depth by binaries is a more difficult issue. Using three different approaches we obtain the values between 3% and 11%.

5 Discussion

Our fitting procedure is based on two important simplifications. First we use mostly a point source model while calculating the source magnification. We make some self consistency checks using also extended source models, but we are not able to fit its size. The effects of source size are important during caustic crossing and/or cusp approaches. Some of the models would have probably been changed if the data were better sampled. Only the event SC36_4030 (1999-BUL-11), for which there are many observations of the second caustic crossing might be used to constrain the source size. The observations near the caustic are, however, marked as not to be trusted by DIA photometry pipeline and we do not include them. The second simplification is the fact that we neglect all effects of the Earth motion, rotation of the binary, and possible acceleration of the source. In fact we have attempted fits including the effects of parallax/acceleration,

but finally we have decided not to use them. Formally for long lasting events the Earth motion should be included. In the case of single lens events, the Einstein time is simply related to the duration of strong amplification. In the case of a binary this is not necessarily so: the passage through or near a small caustic, which implies strong lensing, may last much shorter than the Einstein time. The observations of only weekly magnified source are not discriminating between the models. Thus, even for formally “long” events it is not easy to measure the effects of changes in the relative velocity of the source. Introducing extra parameters describing the relative acceleration of the source may serve as to lower the χ^2 value appreciably (at least for some events), but the extra parameters cannot be well constrained.

The estimates of the caustic size which we use for self consistency checks may also be used to place limits on possible lens mass and luminosity. In some cases the resulting lens brightness is too high. We do not consider this a serious problem, since the relative velocity of the lens may be substantially different from the “typical” value used in the estimates.

For two events (SC20_1793 and SC20_3525) the formally best binary lens models have extreme mass ratios ($q < 0.02$), which may suggest they contain brown dwarfs or Jupiter-like objects. The same events can be, however, modeled using binary lens models with much higher mass ratio, which cannot be rejected with high confidence. Some parts of the parameter confidence region also reach low mass ratio values ($q \approx 10^{-2}$) for SC35_2526, but this is a case of very weakly constrained solutions. Statistically acceptable models may belong to a wide region of mass ratios. Thus we cannot conclude a presence of a planetary system among binary lens candidates.

The distribution of Einstein radius crossing times among the models requires further investigation. The occurrence of long lasting events is certainly more likely in our sample as compared to single lens sample. The same effect but to lesser extent is also present in Alcock *et al.* (2000) sample of binary lens candidates. Since the recognition of binary events requires longer baselines, there is certainly some selection effect involved. The essential part of the light curves – caustic crossings or cusp approach (approaches) may last only a small fraction of the Einstein time. That puts some lower limit on the inter-caustic time, depending on the frequency of observations. With observations made once a day we are biased toward long lasting events.

5.1 Comparison with Previous Study

We are using DIA processed observations of OGLE-II in the direction of Galactic bulge made in seasons 1997–1999 (Woźniak *et al.* 2001). The same observational material, but processed differently, has been analyzed by Udalski *et al.* (2000), who explicitly mark the binary lens candidates in their Table 2. We list all their candidates in our Table 3, and show their status according to the present study.

Four of the Udalski *et al.* (2000) binary lens candidates (see Table 3) are not in the transient database of Woźniak *et al.* (2001), and another one has not

passed our selection criteria. Two of the events were also on the list of our 27 candidates, but have been rejected after the attempt to fit them with binary lens model. In five cases we believe the events are due to single lens rather than binary. (Three cases are strong: the DIA photometry does not show the irregularities of the light curves near maximum, which are present on the plots in the Udalski *et al.* (2000) catalog. Two other cases are examples of noisy light curves and we treat them as poor quality single lens cases.) In nine cases we agree that the events are due to binary lenses, but in two of them we think there is no caustic crossing.

The comparison of our sample with the list of 520 microlensing events of Woźniak *et al.* (2001) is also due, because in both cases the same database has been used. Our approach differs since we apply stronger selection criteria to have a better chance of distinguish the binary lens candidates. The possible binary lens events are not marked in the other study, so a direct comparison is not possible. Of our original 27 binary lens candidates only 3 are missing on the Woźniak *et al.* (2001) list. After attempting to model the 27 candidate events as binary lenses, we reject 9 of them, including the three cases mentioned above. According to our study, the rejected events are not due to microlensing, and this includes 6 cases from the Woźniak *et al.* (2001) list; at the same time the list includes all 18 of our final binary lens candidates. The single lenses have not been studied extensively. Two events, which we classify as single microlensing are missing in the Woźniak *et al.* (2001) sample – these are rather poor cases of microlensed light curves. Two events, which we mark as “other objects” belong to the list of Woźniak *et al.* (2001).

The event SC_21 6195 has been considered also by Alcock *et al.* (2000) (their symbol: 97-BLG-d2.) Both models are qualitatively similar, representing intermediate separation binaries and source trajectory approaching one cusp and then crossing the caustic twice near another cusp. Model parameters differ from 7% (impact parameter) to 40% (mass ratio). The parameter defining blending can not be compared directly because of different filters used by OGLE and MACHO teams.

Acknowledgements. We thank Bohdan Paczyński for many helpful discussions. Special thanks are due to Shude Mao for the permission of using his binary lens modeling software, to Przemek Woźniak for the permission to use DIA photometry transient database before its publication, and to OGLE team for their generous early release of data. This work was supported in part by the Polish KBN grant 2-P03D-013-16 and the NSF grant AST 98-20314.

REFERENCES

- Abt, H.A. 1983, *Ann. Rev. Astron. Astrophys.*, **21**, 343.
 Alard, C. 2000, *Astron. Astrophys. Suppl. Ser.*, **144**, 363.
 Alard, C., and Lupton, R.H. 1998, *Astrophys. J.*, **503**, 325.
 Albrow, M.D., *et al.* 1999a, *Astrophys. J.*, **512**, 672.
 Albrow, M.D., *et al.* 1999b, *Astrophys. J.*, **522**, 1011.

- Albrow, M.D., *et al.* 1999c, *Astrophys. J.*, **522**, 1022.
- Alcock, C., *et al.* 2000, *Astrophys. J.*, **541**, 270.
- An, J.H., *et al.* 2001, *Astrophys. J.*.submitted, astro-ph/0110095
- Blandford, R.D., and Narayan, R. 1992, *Ann. Rev. Astron. Astrophys.*, **30**, 311.
- DiStefano, R., and Mao, S. 1996, *Astrophys. J.*, **457**, 93.
- Dominik, M. 1998, *Astron. Astrophys.*, **333**, L79.
- Dominik, M. 1999, *Astron. Astrophys.*, **341**, 943.
- Jaroszyński, M., and Mao, S. 2001, *MNRAS*, **325**, 1546.
- Mao, S., and DiStefano, R. 1995, *Astrophys. J.*, **440**, 22.
- Mao, S., and Loeb, A. 2001, *Astrophys. J. Letters*, **547**, L97.
- Mao, S., and Paczyński, B. 1991, *Astrophys. J. Letters*, **374**, L37.
- Paczynski, B. 1996, *Ann. Rev. Astron. Astrophys.*, **34**, 419.
- Press W.H., Teukolsky S.A., Vetterling W.T., and Flannery B.P. 1992, in: "Numerical Recipes in Fortran" (NY: CUP).
- Schneider, P., Ehlers, J., and Falco, E.E. 1992, "Gravitational Lenses", Springer, Berlin.
- Schneider, P., and Weiss, A. 1986, *Astron. Astrophys.*, **164**, 237.
- Trimble, V. 1990, *MNRAS*, **242**, 79.
- Udalski, A. *et al.* 1994a, *Astrophys. J. Letters*, **436**, L103.
- Udalski, A., Szymański, M., Kaluzny, J., Kubiak, M., Mateo, M., Krzemiński, W., and Paczyński, B. 1994b, *Acta Astron.*, **44**, 227.
- Udalski, A., Żebruń, K., Szymański, M., Kubiak, M., Pietrzyński, G., Soszyński, I., and Woźniak, P. 2000, *Acta Astron.*, **50**, 1.
- Woźniak, P.R. 2000, *Acta Astron.*, **50**, 421.
- Woźniak, P.R., and Paczyński, B. 1997, *Astrophys. J.*, **487**, 55.
- Woźniak, P.R., Udalski, A., Szymański, M., Kubiak, M., Pietrzyński, G., Soszyński, I., and Żebruń, K. 2001, *Acta Astron.*, **51**, 175.

T a b l e 3
Comparison with previous study

Field	Identification			Remarks	
	OGLE	EWS	DIA	Udalski	This study
BUL_SC3	541151	–	5453	BIN?	SIN
BUL_SC3	590098	–	7783	BCC	not a lens
BUL_SC3	792295	1998-BUL-28	7390	BCC	nCC
BUL_SC15	373196	–	1631	BCC	BCC
BUL_SC16	32304	–	1048	BCC	BCC
BUL_SC19	26606	1999-BUL-23	669	BCC	BCC
BUL_SC19	64524	–	—	BCC	not a transient
BUL_SC20	391296	–	5451	BIN?	SIN
BUL_SC20	395103	–	5875	BIN	not selected
BUL_SC20	708586	1999-BUL-25	3525	BCC	nCC
BUL_SC21	833776	–	6195	BCC	BCC
BUL_SC23	282632	–	2041	BIN?	not a lens
BUL_SC30	352272	–	—	BCC	not a transient
BUL_SC31	293442	1999-BUL-17	1795	BCC	BCC
BUL_SC33	476067	1999-BUL-42	—	BCC	not a transient
BUL_SC34	87132	–	2535	BCC?	SIN
BUL_SC35	305604	–	2526	BCC	BCC
BUL_SC36	336761	1999-BUL-11	4030	BCC	BCC
BUL_SC39	259656	1999-BUL-45	1405	DLS	SIN?
BUL_SC39	378193	–	5900	BIN	SIN?
BUL_SC40	434222	1999-BUL-19	—	DLS	not a transient

Note: The event identification is given in columns 1–4. We repeat the remarks of Udalski *et al.* (2000) in column 5, where the acronyms have the following meaning: BCC – binary lens with caustic crossing, BIN – possible binary lens, and DLS – binary lens or double source star. In column 6 we give our own remarks using also: SIN – single lens, and nCC – binary lens with no caustic crossing. The events not in the transient sample are marked as “not a transient”, and events rejected after modeling as binary lenses – “not a lens”.

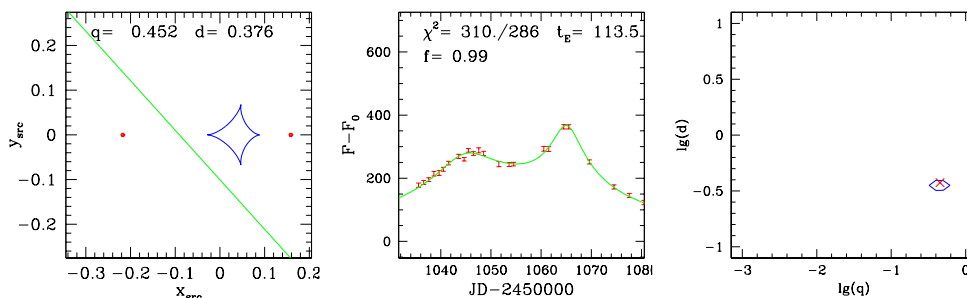
Appendix: The Individual Cases

Binary Lens Candidates According to this Study

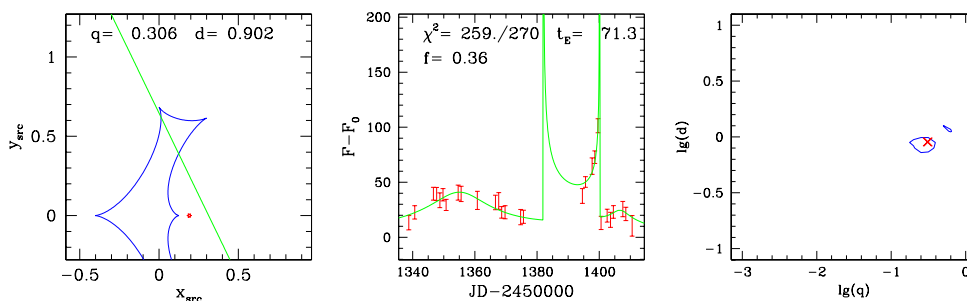
Below we present the plots for the eighteen events which are well explained as caused by the binary lens passage between the source and the observer. The cases are ordered according to the field numbers of the OGLE-II database (Udalski et al. 2000). For each event we give its name as used by Woniak et al. (2001) for transients identified using DIA photometry. For events recognized with the profile photometry, we also give the OGLE star number, and if applicable its EWS name. One of the events (BUL_SC21 833776) is also analyzed by the MACHO group (Alcock et al. 2000) and its name (97-BLG-d2) is also used.

Each case is illustrated with three panels. The most interesting part of the source trajectory, the binary and its caustic structure are shown in the left panel for the best model. The labels give the q and d values. In the middle the part of the best fit light curve is compared with observations. The labels give the χ^2/DOF values. The Einstein time t_E in days and the source flux/base flux ratio $f \equiv F_s/F_{\text{base}}$ are also given. The diagram on the right shows the 68% confidence regions in the $\lg q$ - $\lg d$ plane. The location of the best fit is marked with the cross.

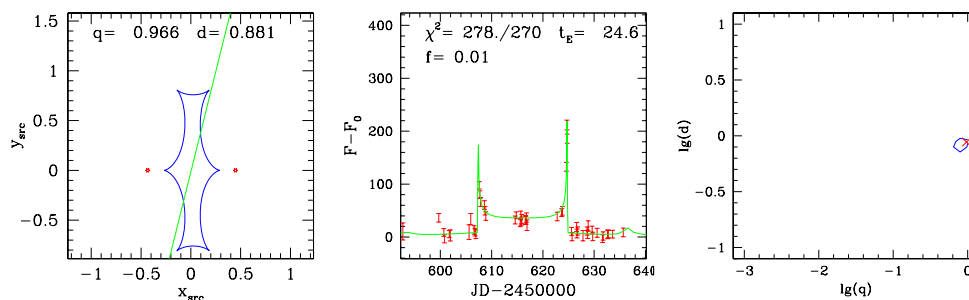
SC3_7390 [BUL_SC3 792295] 1998-BUL-28



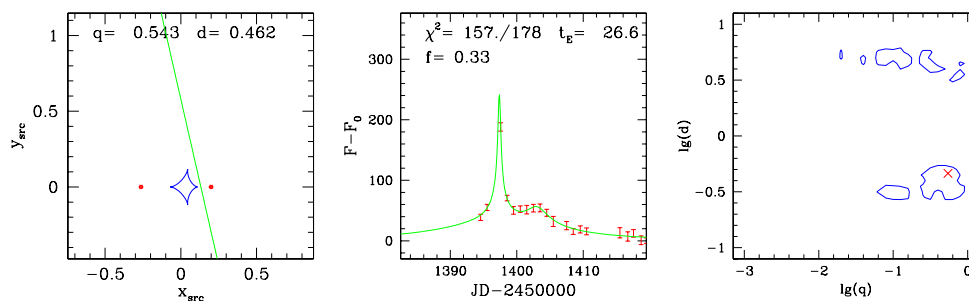
SC4_6350



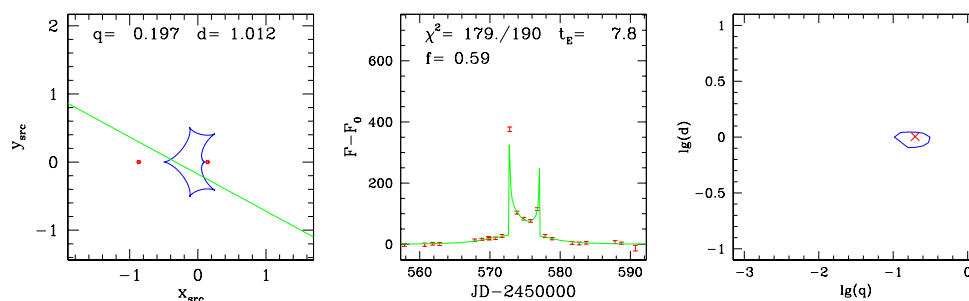
SC5_6550



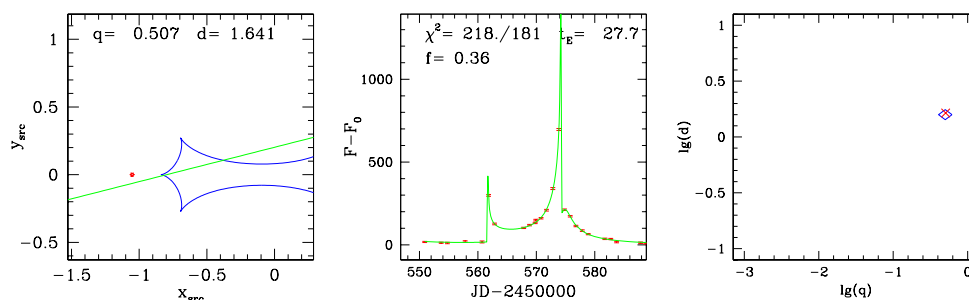
SC12_997



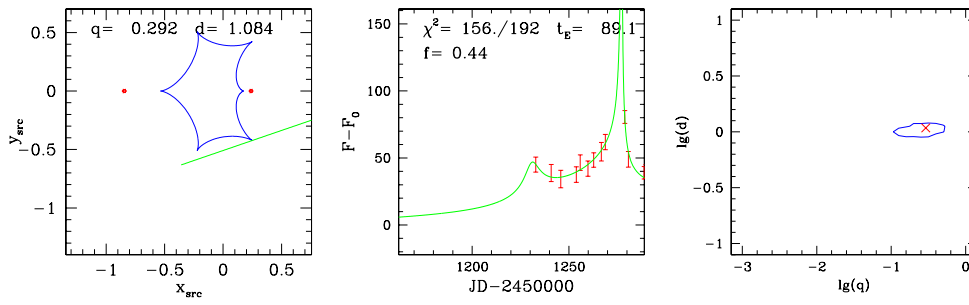
SC15_1631 [BUL_SC15 373196]



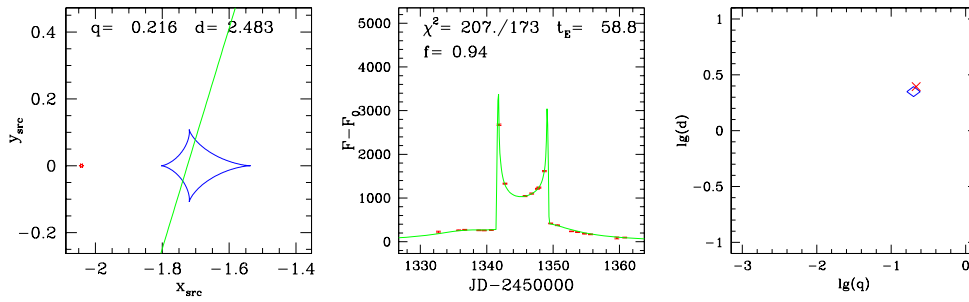
SC16_1047 [BUL_SC16 32304]



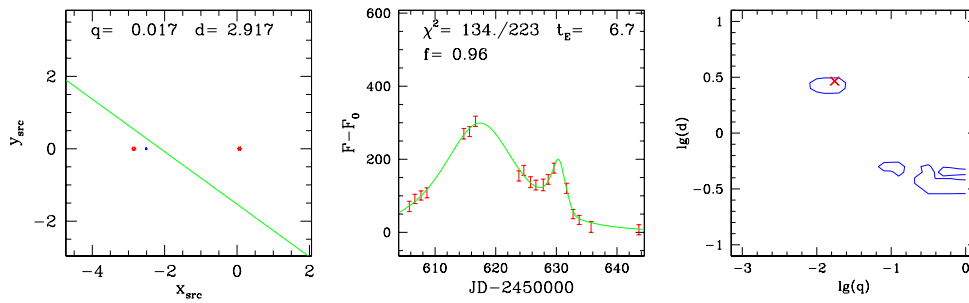
SC18_4924



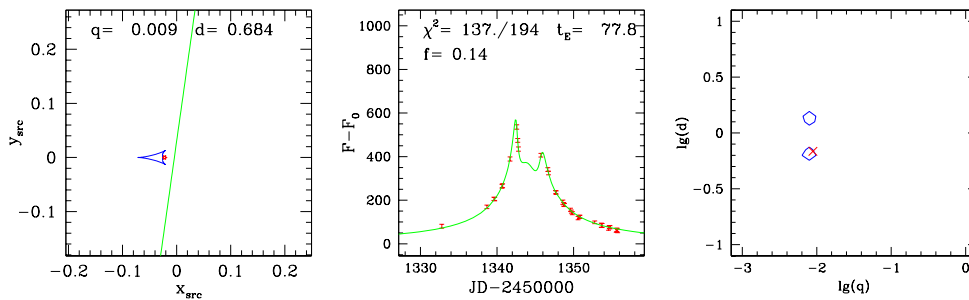
SC19_668 [BUL_SC19 26606] 1999-BUL-23



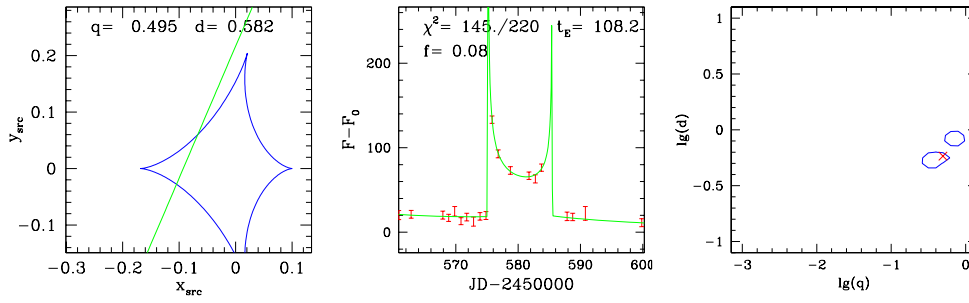
SC20_1793



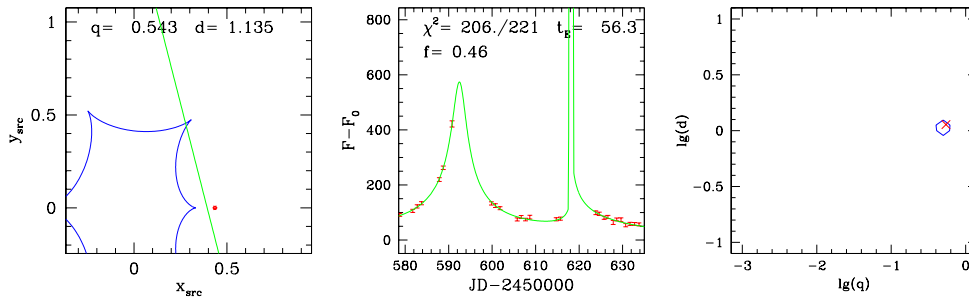
SC20_3525 [BUL_SC20 708586] 1999-BUL-25



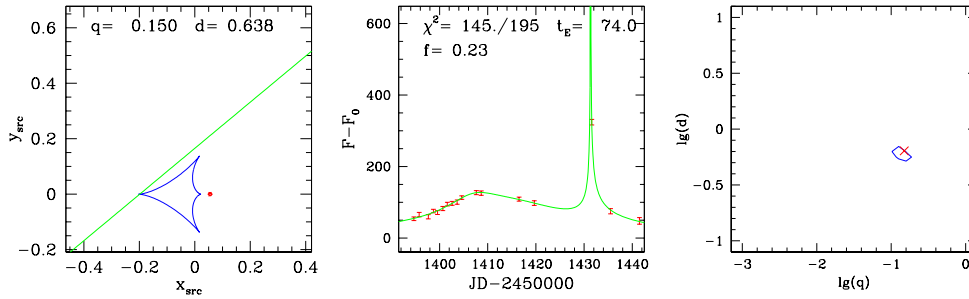
SC20_4694



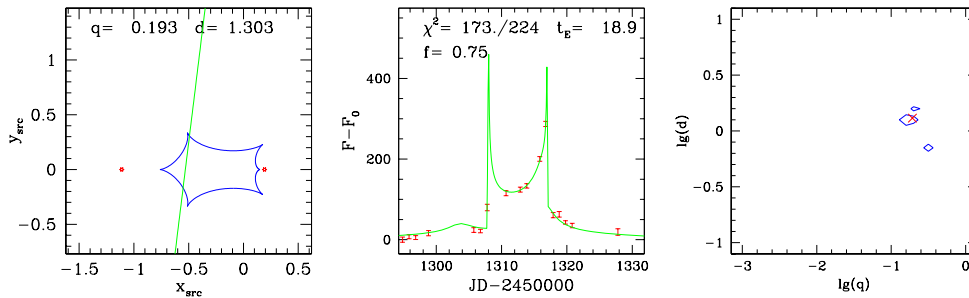
SC21_6195 [BUL_SC21 833776] (97-BLG-d2)



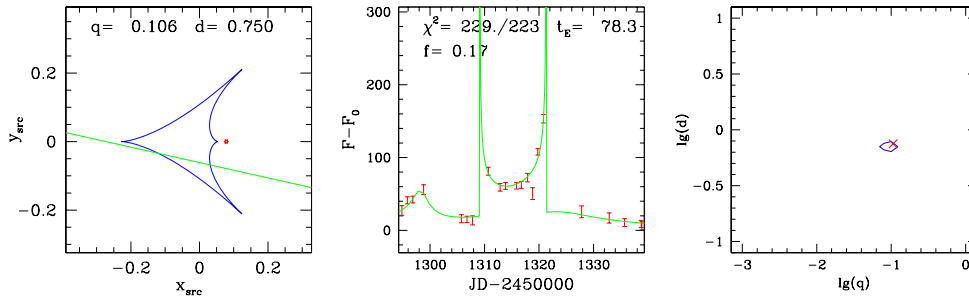
SC30_4491



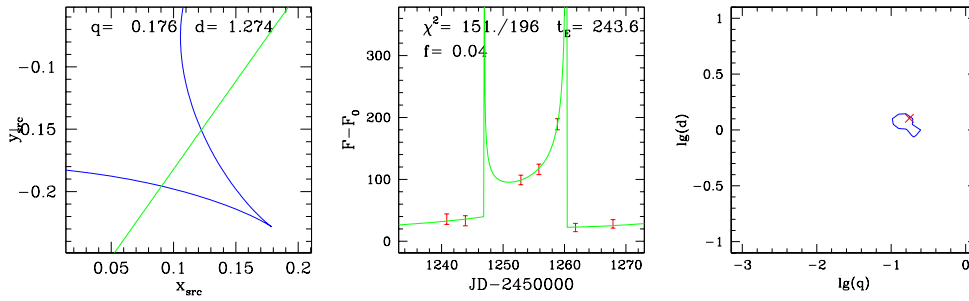
SC31_1795 [BUL_SC31 293442] 1999-BUL-17



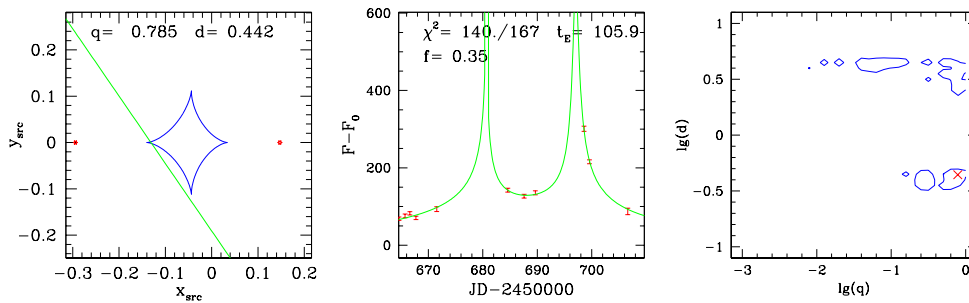
SC31_3204



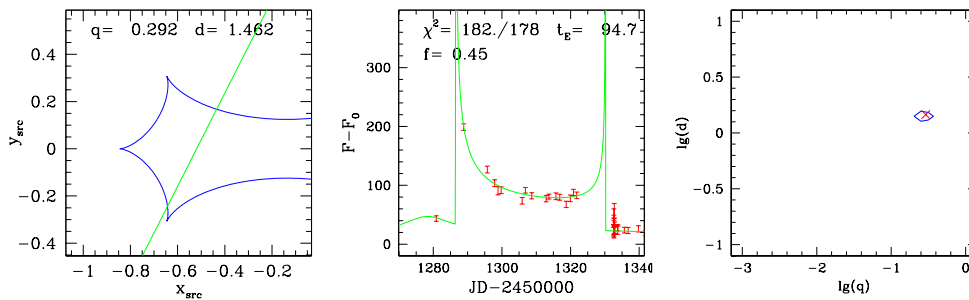
SC32_4683



SC35_2526 [BUL_SC35 305604]



SC36_4030 [BUL_SC36 336761] 1999-BUL-11



Rejected Events

Below we present the attempted fits using binary lens model for the remaining events. These do not represent the genuine binary lens candidates but rather some internal variability of the source.

